#To the respected reviewer 1

We thank the reviewer for the constructive comments that help improve the presentation of the original manuscript. Below are our point-to-point replies to the reviewer's comments (original comments are in italics):

Main points:

1. The only reference to the Pacific-Indian Ocean Associated Mode I can find is related to a few publications by the authors themselves. Essentially, what is meant by this Mode is the well-known teleconnection between the Pacific (ENSO) and the Indian Ocean. Unfortunately, this study even fails to take the seasonality of this teleconnection into account. For example, in boreal winter the main mode of variability of the Indian ocean (the basin mode) is forced by ENSO, whereas in summer and autumn the response of the Indian Ocean to ENSO projects onto the IOD (which is the focus of this study). However, this seasonality is important but not addressed at all. For example, this basin mode can be seen in Fig. 1, whereas the IOD response may be identified in Fig. 6. To not consider this seasonality makes the study essentially useless.

Reply: Thank you for your comment very much. We followed the suggestion that seasonality is needed to be considered, and thank the specialist for precious advice. The Pacific-Indian Ocean associated mode (PIOAM), defined as the first dominant mode (empirical orthogonal function, EOF1) of SST anomalies in the Pacific-Indian Ocean between 20°S and 20°N. Figure below shows the pattern of SST anomalies over the Indo-Pacific Ocean in October 1982 and September 1997. It can be clearly seen that there are obvious warm tongues in the eastern equatorial Pacific Ocean, obvious positive SST anomalies in the northwest Indian Ocean, and obvious negative SST anomalies in the western equatorial Pacific Ocean and the eastern Indian Ocean. This is precisely the typical spatial pattern characteristics of the PIOAM. That is to say, the SST anomalies in the northwest Indian Ocean and the equatorial middle-east Pacific Ocean is opposite to the SST anomalies in the western equatorial Pacific Ocean and the east Indian Ocean. Compared with ENSO and IOD, the PIOAM has a broader spatial distribution.

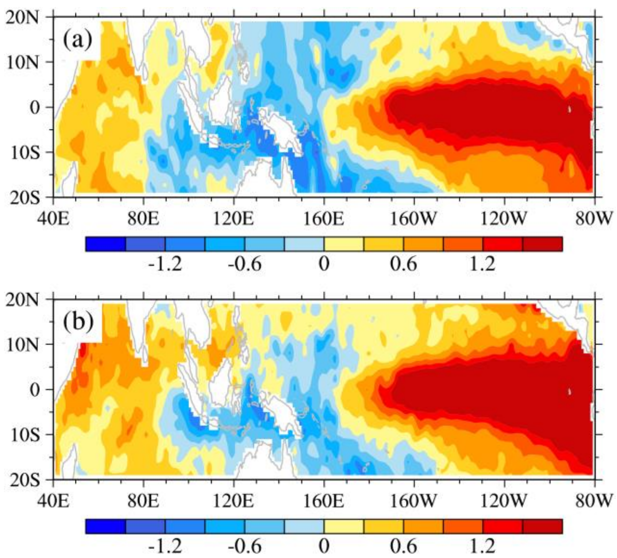

Maps of SST anomalies for (a) October 1982 and (b) September 1997 from the HadISST dataset (unit: °C). The period from 1981 to 2005 is used to extract the monthly SST climatology.

However, is this spatial pattern of SST anomalies only a special case of a certain year, or is it stable? To answer this question, EOF analysis is performed on the SST anomalies of different seasons over Indo-Pacific Ocean (20°S-20°N, 40°E-80W°) from 1951 to 2005. All these first leading modes in Figure below are well separated from the remaining leading modes, based on the criteria of North et al. (1982), which means less likely to be affected by statistical sampling errors. It can be found that the patterns of summer (June, July and August; Figure below b) and autumn (September, October and November; Figure below c) display the typical spatial distribution of the PIOAM, with the 46% and 61% contribution to total variance, respectively, while the spatial pattern of PIOAM is not so obvious in spring (March, April and May; Figure below a) and winter (December, January and February; Figure below d). In general, the PIOAM has stable structure and practical significance, especially in autumn.

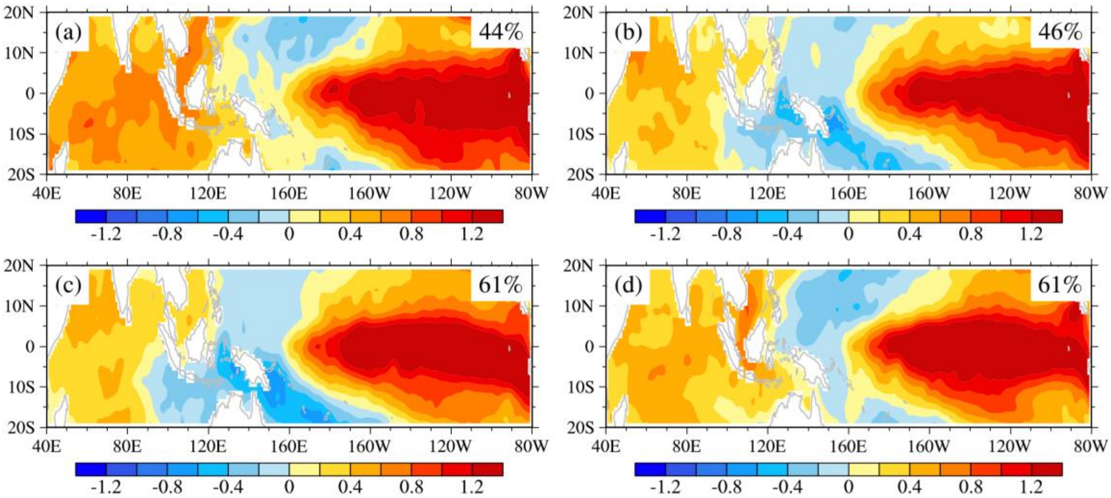

Spatial patterns of the first leading mode of the (a) spring (March, April and May), (b) summer (June, July and August), (c) autumn (September, October and November) and (d) winter (December, January and February) averaged SST anomalies over Indo-Pacific Ocean (20°S-20°N, 40°E-80W°) calculated from HadISST dataset (unit: °C). The numbers at the upper right corner of each panel indicate the percentage of variance explained by each season.

In addition, based on multi-variable empirical orthogonal functions, Chen and Cane (2008) and Chen (2011) also found this phenomenon and named it Indo-Pacific Tripole (IPT), which is considered to be an intrinsic mode in the tropical Indo-Pacific Ocean. In addition, Lian et al. (2014) used a conceptual model to discuss the development and physical mechanism of the IPT. Yang et al. (2006) found that the influences of the PIOAM and the ENSO mode on summer precipitation and climate in China were very different, and their numerical experiments also showed that the simulation results obtained by considering the PIOAM were more consistent with observation data. Therefore, evaluating and improving the capability of current climate models to simulate the PIOAM are beneficial to obtain accurate climate predictions.

Please see lines 8-10, 75-79 and 133-162.

Reference:

Chen, D., Cane, M. A.: El Niño prediction and predictability, J. Comput. Phys., 227, 3625-3640, doi: 10.1016/j.jcp.2007.05.014, 2008.

Chen, D.: Indo-Pacific Tripole: An intrinsic mode of tropical climate variability, Adv. Geosci., 24, 1-18, doi: 10.1142/9789814355353_0001, 2011.

Lian, T., Chen, D. K., Tang, Y. M., Jin, B. G.: A theoretical investigation of the tropical Indo-Pacific tripole mode, Sci. China-Earth Sci., 57, 174-188, doi: 10.1007/s11430-013-4762-7, 2014.

North G. R., Bell, T. L., Cahalan, R. F., Moeng, F. J.: Sampling errors in the estimation of empirical orthogonal functions, Mon. Wea. Rev., 110, 699-706, doi: 10.1175/1520-0493(1982)110<0699:seiteo>2.0.co;2, 1982.

Yang, H., Jia, X. L. and Li, C. Y.: The tropical Pacific-Indian Ocean temperature anomaly mode and its effect, Chin. Sci. Bull., 51(23): 2878-2884, doi:10.1007/s11434-006-2199-5, 2006.

2. The ad-hoc definition in Eqs. 1,2,3 is not good enough. The common Indo-Pacific mode should be identified by an EOF analysis.

Reply: Thank you for your comment very much. It is customary to select the time coefficient (PC1) of the PIOAM as its index. It can be seen from the regression of the monthly SSTA onto the normalized PC1 (Figure below a) that the pattern in the Pacific Ocean is similar to ENSO, but positive SST anomalies occur throughout the Indian Ocean, which not matches the typical PIOAM spatial pattern. This is because the ENSO signals in the Pacific Ocean in PC1 are so strong that the signals of the IOD are not fully reflected. The correlation coefficient between PC1 and Niño3.4 index is as high as 0.95. However, obvious negative SST anomalies in the eastern Indian Ocean can be found in the regression map of the monthly SSTA based on the normalized PIOAMI (Figure below b) defined by Eqs. 1, 2, 3. The correlation coefficient between PIOAMI and Niño3.4 index is 0.68, indicating PIOAMI contains more Indian Ocean signals than PC1. In addition, the correlation coefficient between PC1 and PIOAMI is 0.70, which is far more than the confidence level of 99%. Therefore, PIOAMI can describe the mode well because of giving consideration to both the signals in the Pacific Ocean and the signals in the Indian Ocean.

Please see lines 254-269.

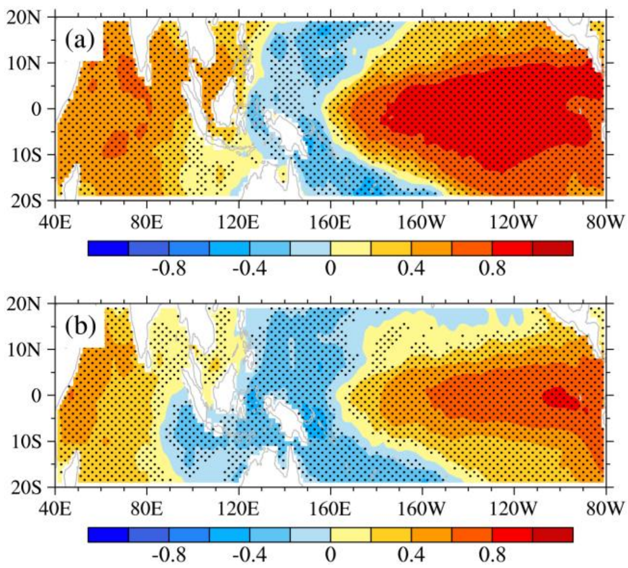

Regressions of the monthly SSTA onto the normalized (a) PC1 and (b) PIOAMI for the period from

1951 to 2005 (unit: ℃). The stippled areas for SSTA denote the 99% confidence levels.

3. There is no in-depth analysis as to why the models do or do not represent the mode. Section 4 is pure speculation. The fact that some models including carbon cycle simulate the mode slightly better does not proof anything, if not supported by a large number of models, or by dedicated experiments.

Reply: Thank you for your comment very much. We think your suggestion is correct and delete the Section 4 which is based on most of the speculation. The abstract and discussion are also be revised.

Please see lines 23-25, 369-412 and 443-453.

#To the respected Ian G. Watterson

We thank the reviewer for the constructive comments that help improve the presentation of the original manuscript. Below are our point-to-point replies to the reviewer's comments (original comments are in italics):

General comments: This is an interesting analysis of the tropical ocean surface temperatures from CMIP5 and HadISST. A 'mode' derived from the tropical Pacific-Indian domain has been denoted the PIOAM by some previous authors, mostly in Chinese journals. It seems worthwhile introducing the approach to this European one.

Here, it is shown that this Pacific-Indian mode (presumably obtained by principal component analysis) from 21 CMIP5 models has much in common with that from observations. There is a lengthy description of the differences among models. The mode is loosely linked to the IOD and ENSO, in section 3.1 of the study. The analysis in section 3.2 focuses on alternative IOI and POI indices. A major problem is that a further index PIOAMI is then used as though it is the same as the first one (presumably PC1). Section 4 attempts to relate the differences between models to their differences in formulation. However, this is unconvincing, especially as there is no estimation of statistical uncertainty in results that have been obtained from a single 55-year period. Some conclusions are not well supported. I initially thought the index might be linked to a 'Pacific-Indian Dipole' that I have used in analysing CMIP5 future climate simulations (see two recent references, below). However, the boxes used in that PID are a little shifted in longitude, so I expect there is only a weak relationship. Nevertheless, it might be worthwhile mentioning that alternative P-I index, and the shift.

The presentation in the paper is superficially quite good. However, there are many important details that are omitted, including in the captions. The 30 points listed below provide some guide to how the presentation needs to be improved. The major problem of having multiple indices, with no statistical uncertainty attached, will need to be overcome before final publication can be considered.

Significant points (at Line numbers):

1. L8-9 This needs to be a more helpful definition of how the PIOAM mode is defined, given that it is a rather new term.

Reply: Thank you for your suggestion. We have given the definition PIOAM in the abstract, which helps the reader to see our work more directly.

Please see lines 8-10.

2. L13 Why is HadISST referred to as a reanalysis? I don't think the Met Office does.

Reply: Thank you for your comment. We have corrected it, replacing 'reanalysis' with 'dataset' throughout the revised manuscript.

3. L46 Walker needs to have a capital W, as it is a person's name -in several places

Reply: Thank you for your reminding. Done.

Please see lines 47, 60 and 61.

4. L96 What CMIP5 simulations are used? Historical?

Reply: Thank you for your reminding. Yes, it's historical, and we've added that.

Please see line 101.

5. L101 Table 1 'oceanic resolution' might not be accurate given some have higher resolution in tropics. Is this the grid for the available ocean data?

Reply: Thank you for your comment. We directly get the resolution of each model from the downloaded data, as showed below. In view of the resolution in tropical regions, we have supplemented it in the article.

Please see lines 102-103.

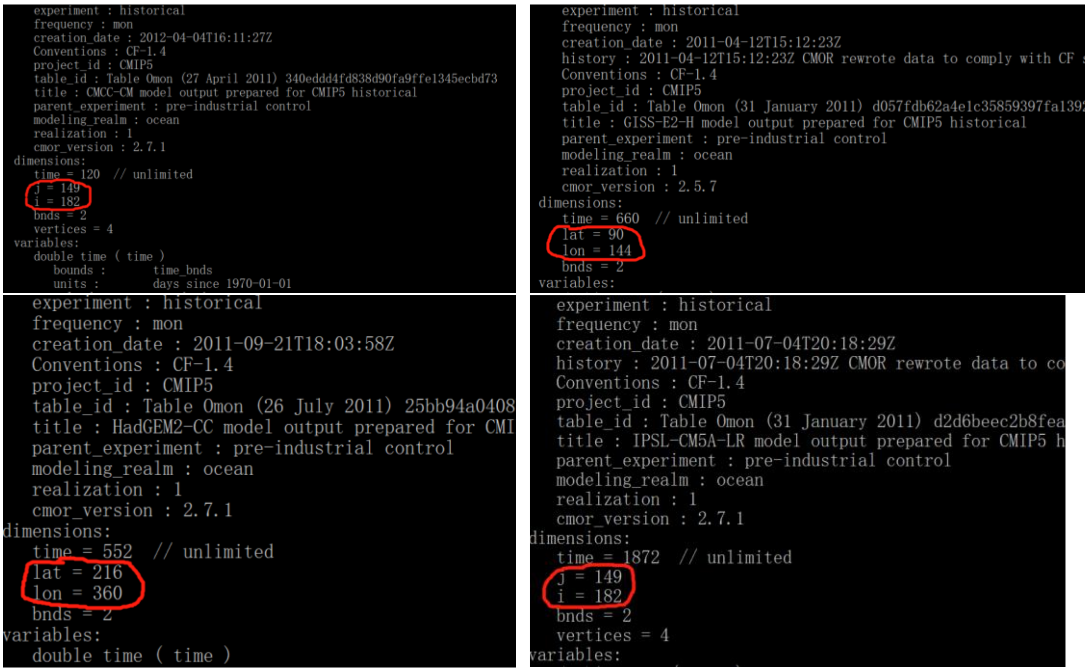

```
   experiment : historical
   frequency : mon
   creation_date : 2012-04-04T16:11:27Z
   Conventions : CF-1.4
   project_id : CMIP5
   table_id : Table Omon (27 April 2011) 340eddd4fd838d90fa9ffe1345ecbd73
   title : CMCC-CM model output prepared for CMIP5 historical
   parent_experiment : pre-industrial control
   modeling_realm : ocean
   realization : 1
   cmor_version : 2.7.1
dimensions:
   time = 120  // unlimited
   j = 149
   i = 182
   bnds = 2
   vertices = 4
variables:
   double time ( time )
      bounds :        time_bnds
      units :         days since 1970-01-01
```

```
   experiment : historical
   frequency : mon
   creation_date : 2011-04-12T15:12:23Z
   history : 2011-04-12T15:12:23Z CMOR rewrote data to comply with CF
   Conventions : CF-1.4
   project_id : CMIP5
   table_id : Table Omon (31 January 2011) d057fdb62a4e1c35859397fa139
   title : GISS-E2-H model output prepared for CMIP5 historical
   parent_experiment : pre-industrial control
   modeling_realm : ocean
   realization : 1
   cmor_version : 2.5.7
dimensions:
   time = 660  // unlimited
   lat = 90
   lon = 144
   bnds = 2
variables:
```

```
   experiment : historical
   frequency : mon
   creation_date : 2011-09-21T18:03:58Z
   Conventions : CF-1.4
   project_id : CMIP5
   table_id : Table Omon (26 July 2011) 25bb94a0408
   title : HadGEM2-CC model output prepared for CMI
   parent_experiment : pre-industrial control
   modeling_realm : ocean
   realization : 1
   cmor_version : 2.7.1
dimensions:
   time = 552  // unlimited
   lat = 216
   lon = 360
   bnds = 2
variables:
   double time ( time )
```

```
   experiment : historical
   frequency : mon
   creation_date : 2011-07-04T20:18:29Z
   history : 2011-07-04T20:18:29Z CMOR rewrote data to co
   Conventions : CF-1.4
   project_id : CMIP5
   table_id : Table Omon (31 January 2011) d2d6beec2b8fea
   title : IPSL-CM5A-LR model output prepared for CMIP5 h
   parent_experiment : pre-industrial control
   modeling_realm : ocean
   realization : 1
   cmor_version : 2.7.1
dimensions:
   time = 1872  // unlimited
   j = 149
   i = 182
   bnds = 2
   vertices = 4
variables:
```

6. L104 'Tropics' is normally considered bounded by 23 degrees latitude. Plot 1 shows 20S-20N. Which is used here? What are the longitudinal bounds?

Reply: Thank you for your comment very much. The 'Tropics' we are talking about here is to distinguish from the mid-latitudes. When it comes to computing, we use 20°S -20°N. I'm sorry we didn't mention longitudinal bounds. It's 40°E -80°W. It has been added in the revised manuscript.

Please see line 110.

7. L104 Is the analysis done on anomalies around a mean annual cycle? Is the data detrended?

Reply: Thank you for your comment. We removed the annual cycle and the linear trend before performing the EOF on the tropical Pacific-Indian ocean SSTA. It has been supplemented in this article.

Please see lines 110-111.

8. L108 How is this 'mode' calculated? I presume it is a principal component/EOF analysis. The interval of Fig 1, 0.003C makes this seem a very small amplitude. Could these EOF1 fields be scaled so they show the temperature anomaly for a 1 standard deviation of the index or PC1? Do the *differences look the same?*

Reply: Thank you for your comment very much. This mode is obtained by EOF analysis, and we have added additional explanation in the article. The Figure 1 with the interval 0.003℃ is the direct results of EOF analysis. However, the amplitude of this pattern is relatively small. After scaling the patterns of this mode by normalizing the PC1 of each model and HadISST data set, the Figure 1 is redrawn with the interval 0.2℃. The distributions of differences are in accordance with previous results.

Please see lines 206-211.

9. L119 Error in longitudes for POI -should be 80W not 80E

Reply: Thank you very much. It has been corrected.

Please see line 126.

10. L137 is rather late to state 'so-called'!

Reply: Thank you very much. It has been corrected.

Please see line 177.

11. L138 What depth does heat refer to?

Reply: Thank you for your comment. It refers to the surface, and it has been added.

Please see lines 178.

12. L138-140 This needs more discussion, perhaps earlier. What is the mathematical meaning? Should 'presents' be 'represents'?

Reply: Thank you for your comment very much. This sentence does not correspond to what we are actually trying to convey. What we want to say is that the IOD is also like a meridional seesaw, and the text has been reworded.

Please see lines 179-181.

13. L143 What is the statistical uncertainty of this analysis? There are only 55 years, or 20 ENSO cycles, perhaps. It would be good to obtain additional simulations from at least one model to give some indication.

Reply: Thank you for your comment very much. Because EOF analysis is used here to capture the pattern of PIOAM rather than composite analysis (Liu et al. 2013; Zhang and Sun 2014) or regression analysis (Jha et al. 2014; Chen et al. 2017; Chen et al. 2019), statistical significance test cannot be performed in Figure 1, which can also be seen in other studies (i.e. the North Pacific Oscillation in Wang et al. (2019), the Pacific Decadal Oscillation in Lin et al. (2018), the interdecadal variability of SST in Lyu et al. (2016), the IOD and ENSO in Weller and Cai (2013)). Actually, the spatial correlation coefficients of the pattern of PIOAM between the HadISST and each CMIP5 model (in Figure 2) have significance at 99% confidence level. In addition, the first leading mode (PIOAM) is well separated from the remaining leading modes, based on the criteria of North et al. (1982), which means less likely to be affected by statistical sampling errors.

Please see lines 167-169.

Reference:

Chen S, Wu R, Chen W, Song L. (2019) Performance of the CMIP5 models in simulating the Arctic Oscillation during boreal spring. Clim. Dyn. Doi: 10.1007/s00382-019-04792-3

Chen S, Chen W, Yu B. (2017) The influence of boreal spring Arctic Oscillation on the subsequent winter ENSO in CMIP5 models. Clim. Dyn. Doi: 10.1007/s00382-016-3243-z

Liu L, Xie SP, Zheng XT, Li T, Du Y, Huang G, Yu WD (2013) Indian Ocean variability in the CMIP5 multi-model ensemble: the zonal dipole mode. Clim. Dyn. Doi: 10.1007/s00382-013-2000-9

Lyu K, Zhang X, Church JA, Hu J. (2016) Evaluation of the interdecadal variability of sea surface temperature and sea level in the Pacific in CMIP3 and CMIP5 models. Int. J. Climatol. Doi: 10.1002/joc.4587

Lin R, Zheng F, Dong X. (2018) ENSO Frequency Asymmetry and the Pacific Decadal Oscillation in Observations and 19 CMIP5 Models. Adv. Atmos. Sci. Doi: 10.1007/s00376-017-7133-z

North G. R., Bell, T. L., Cahalan, R. F., Moeng, F. J. (1982) Sampling errors in the estimation of empirical orthogonal functions, Mon. Wea. Rev. Doi: 10.1175/1520-0493(1982)110<0699:seiteo>2.0.co;2

Weller E, Cai W. (2013) Asymmetry in the IOD and ENSO Teleconnection in a CMIP5 Model Ensemble and Its Relevance to Regional Rainfall. J. Clim. Doi: 10.1175/JCLI-D-12-00789.1

Wang X, Chen M, Wang C, Yeh SW, Tan W. (2019) Evaluation of performance of CMIP5 models in simulating the North Pacific Oscillation and El Niño Modoki. Clim. Dyn. Doi: 10.1007/s00382-018-4196-1

Zhang T, Sun DZ. (2014) ENSO Asymmetry in CMIP5 Models. J. Clim. Doi: 10.1175/JCLI-D-13-00454.1

14. L152 where is the ENSO mode shown?

Reply: Thank you for your comment. We mean that the spatial distribution of PIOAM in the Pacific Ocean is similar to ENSO model, which should be expressed as ENSO-like mode rather than ENSO mode. It has been revised.

Please see lines 193, 217 and 305.

15. L163-4 what does this mean?

Reply: Thank you for your comment. We want to briefly describe the PIOAM in MME. This sentence has been rewritten as ‘MME better simulates the amplitude of PIOAM in the Indian Ocean than most these selected CMIP5 models with smaller simulation errors, but the amplitude in the equatorial Pacific are larger than that of the HadISST dataset’, which may not be that confusing caused by our inappropriate expressions.

Please see lines 203-205.

16. L167 In the Fig 1 caption what is the % value?

Reply: Thank you for your comment. I'm sorry we overlooked it. The numbers at the upper right corner of each panel indicate the percentage of variance explained by each model. It has been added to the caption of Figure 1.

Please see lines 210-211.

17. L170 where is the IOD mode shown?

Reply: Thank you for your comment. This is similar to the previous question which concerns ENSO mode. We want to express the pattern of PIOAM in the Indian Ocean is similar to IOD mode. We have replaced the IOD mode with IOD-like mode.

Please see lines 213 and 305.

18. L192 It is confusing to have 'MME' of three models. What is MME at L193 and later in the paper?

Reply: Thank you for your comment. The MME in this article is multi-model ensemble and Its explanation is given in Section 3.1. The original L192 has been rephrased by deleting 'of these models' to avoid confusing expressions.

Please see line 234.

19. L197 What is Fig. 2 actually showing? Comparisons of EOF1? What is REF?

Reply: Thank you for your comment. The Taylor diagram presented in Figure 2 shows the ratio of the standard deviation calculated from simulation to that obtained in HadISST, spatial correlation coefficient and root mean square error (RMSE). The closer the point representing the model to REF, the better capability of the model. Actually, REF is a reference point. More detailed information of Taylor diagram can be found in Taylor (2001).

Reference:

Taylor, KE. (2001) Summarizing multiple aspects of model performance in a single diagram. J. Geophys. Res. Atmos. Doi:10.1029/2000jd900719.

20. L208 It would seem essential to compare the PC1 of PIOAM with this alternative PIOAMI index. If they are different, then the rest of the paper is misleading, whenever it compares 'PIOAM' with IOD, Nino34 etc. Is the PC1 more closely related to NINO34?

Reply: Thank you for your comment very much. In fact, since SST anomaly changes in the Indian Ocean are not as robust as those in the equatorial eastern Pacific Ocean, ENSO signals in the Pacific Ocean in PC1 are so strong that the signals of the IOD are not fully reflected, which can also be seen in the first picture (Figure a) below. However, PIOAMI can describe the mode well (Figure b), because this selected index takes into account both the signals in the Pacific Ocean and the signals in the Indian Ocean. In addition, the correlation coefficient between PC1 and PIOAMI is 0.70, which is far more than the confidence level of 99%. The correlation coefficients between Nino3.4 and PC1 and PIAOMI are 0.95 and 0.68, respectively, indicating that PC1 is indeed more closely related to Nino3.4.

Please see lines 254-269.

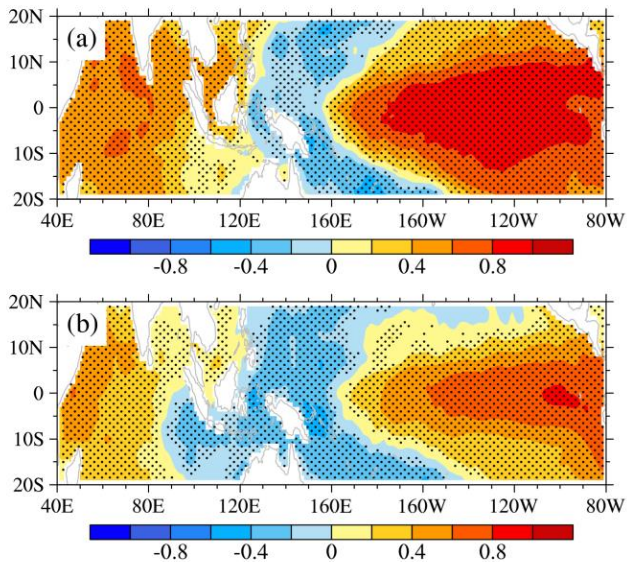

Regressions of the monthly SSTA onto the normalized (a) PC1 and (b) PIOAMI for the period from 1951 to 2005. The stippled areas for SSTA denote the 99% confidence levels.

21. L225 What is 'autumn' for a tropical index? 'Boreal', and September-November perhaps?

Reply: Thank you for your comment. Autumn refers to September, October and November, which we have supplemented in the revised manuscript.

Please see line 284.

22. L225-6 needs to be better written. Is this 1SD a criterion?

Reply: Thank you for your suggestion. Yes, it is. we use one standard deviation as the criterion. This sentence has been rewritten.

Please see lines 285-286.

23. L239 The asymmetry in Fig 5 seems surprising. Does it indicate the index is not a 'normal' distribution?

Reply: Thank you for your comment. We think the CMIP5 models have different performance to capture the PIOAM in different phase, which causes this obvious asymmetry.

24. L243 A composite, perhaps?

Reply: Thank you for your suggestion. Done.

Please see line 302.

25. L255 Is this PIOAM or PIOAMI -here and later?

Reply: Thank you for your comment. We apologize for the confusion. It should be PIOAMI when concerning other indices, like IOI, POI and Niño3.4 index. We have revised and unified it.

Please see line 328.

26. L256 Why is it interesting to show a standard deviation, when the IOI and POI are normalised (L120)? How does this impact the interannual autumn values?

Reply: Thank you for your comment very much. Here we calculated standard deviation to evaluate the ability of these CMIP5 models to simulate the interannual variation of the PIOAM. The closer the ratio is to 1, the better the ability to simulate interannual variation. Yes, it is. We normalized the IOI and POI in Section 2. Considering that PIOAMI is composed of IOI and POI, the interannual variations of IOI and POI may have an impact on PIOAMI, which may involve the internal process of PIOAM and needs further in-depth study.

27. L280 How is IOD defined here? Is it similar to IOI?

Reply: Thank you for your comment. We're sorry we didn't make it clear. Here the IOD is according to the definition of Saji et al. (1999), the difference in SSTA between the tropical western Indian Ocean (50°E-70°E, 10°S-10°N) and the tropical south-eastern Indian Ocean (90°E-110°E, 10°S-0), not it similar to IOI. It has been supplemented in the revised manuscript. Please see lines 342-344.

28. L316 This comparison needs to allow for statistical uncertainty, which should be considered early in the study. Would the results be the same if a different set of simulations is considered?

Reply: Thank you for your comment very much. We delete the Section 4 which is based on most of the speculation because the meaningful conclusions need to be supported by a large number of models, or by dedicated experiments. The abstract and discussion are also be revised.

Please see lines 23-25, 369-412 and 443-453.

29. L325, L337 these statements are not convincingly proved.

Reply: Thank you for your comment.

30. L339. What is the chemical process?

Reply: Thank you for your comment.

Possible references:

Watterson IG (2019) Influence of sea surface temperature on simulated future change in extreme rainfall in the Asia-Pacific. On-line, Asia-Pacific J. Atmos. Sci. doi 10.1007/s13143-019-00141-w

Watterson IG (2019) Indices of climate change based on patterns from CMIP5 models, and the range of projections. Climate Dynamics, 52, 2451-2466, doi 10.1007/s00382-018-4260-x

The Pacific-Indian Ocean Associated Mode in CMIP5 Models

Minghao Yang, Xin Li*, Weilai Shi, Chao Zhang, Jianqi Zhang

College of Meteorology and Oceanography, National University of Defense Technology, Nanjing, 211101, China

Correspondence to: Xin Li (lixin_atocean@sina.cn)

Abstract. The Pacific-Indian Ocean associated mode (PIOAM), defined as the first dominant mode (empirical orthogonal function, EOF1) of SST anomalies in the Pacific-Indian Ocean between 20°S and 20°N, is the product of the tropical air-sea interaction at the cross-basin scale and the main mode of ocean variation in the tropics. Evaluating the capability of current climate models to simulate the PIOAM and finding the possible factors that affect the simulation results are beneficial to obtain more accurate future climate change prediction. Based on 55-yr the Hadley Centre Global Sea Ice and Sea Surface Temperature (HadISST) dataset and the output data from twenty-one Coupled Model Intercomparison Project (CMIP) phase 5 (CMIP5) models, the PIOAM in these CMIP5 models is assessed. It is found that the explained variance of PIOAM in almost all twenty-one CMIP5 models are underestimated. Although all models reproduce the spatial pattern of the positive sea surface temperature anomaly in the eastern equatorial Pacific well, only one-third of these models successfully simulate the ENSO mode with the east-west inverse phase in the Pacific Ocean. In general, CCSM4, GFDL-ESM2M and CMCC-CMS have a stronger capability to capture the PIOAM than that of the other models. The strengths of the PIOAM in the positive phase in less than one-fifth of the models are slightly stronger, and very close to HadISST dataset, especially in CCSM4. The interannual variation of PIOAM can be measured by CCSM4, GISS-E2-R and FGOALS-s2. ~~Further analysis indicates that considering the carbon cycle, resolving stratosphere, chemical process or increasing the horizontal resolution of the atmospheric model may effectively improve the performance of the model to simulate the PIOAM.~~

1. Introduction

As early as the 1960s, Bjerkness (1966, 1969) studied the phenomenon of El Niño-Southern Oscillation (ENSO). Since then, the impact of ENSO on global climate has become a major concern in climate research. ENSO in the Pacific Ocean is the strongest interannual signal of global climate change, and has been extensively studied by a large number of scholars, including its occurrence and development mechanism (Wyrtki, 1975; Philander et al., 1984; Suarez and Schopf, 1988; Jin, 1997; Li and Mu, 1999; Li and Mu, 2000; Li, 2002), its evolution characteristics and its impact on global weather and climate (Bjerknes, 1966; Rasmusson and Wallace, 1983; Ropelewski and Halpert, 1987; Li, 1990; Webster and Yang, 1992; Zhou and Zeng, 2001; Mu and Duan, 2003; Mu et al., 2007; Zheng et al., 2007). At the end of the 20th century, an interannual climate anomaly characterized by a sea surface temperature anomaly (SSTA) of opposing sign in the western and eastern tropical Indian Ocean, known as the Indian Ocean dipole (IOD), was reported by Saji et al. (1999) and Webster et al. (1999) and was catalogued as one of the major ocean-atmosphere coupled phenomena. The SSTA in the tropical Indian Ocean subsequently has been widely studied, and a great deal of literature has discussed the causes and mechanisms of the IOD, as well as its weather and climate impacts (Li and Mu, 2001; Li et al., 2003; Saji and Yamagata, 2003; Cai et al., 2005; Rao et al., 2007; Zheng et al., 2013; Wang and Wang, 2014).

IOD was initially thought to be generated only by independent air-sea interactions in the tropical Indian Ocean, but some studies have suggested that the tropical Indian Ocean SSTA in 1997/1998 was caused by the influence of the ENSO event in the Pacific Ocean on the surface wind field of the Indian Ocean through anti-Walker circulation over the equator, thus causing the SSTA in the Indian Ocean (Yu and Rienecker, 1999). It has also been suggested that the east-west asymmetry anomaly of the Indian Ocean SSTA in 1997/1998 may contain the triggering process of ENSO (Ueda and Matsumoto, 2000). Li et al. (2002) showed that there is a significant negative correlation between the tropical Indian Ocean SSTA dipole event and the Pacific SSTA dipole event (similar to ENSO mode) using statistical analysis. Huang and Kinter (2002) also noted that there was a significant relationship between IOD in the Indian Ocean and ENSO in the Pacific Ocean.

The movements and changes of Earth's fluids (atmosphere and oceans) have a certain connection, and the change in tropical sea surface temperature (SST) should not be an isolated phenomenon. IOD in the Indian Ocean and ENSO in the Pacific Ocean, both as significant basin-scale signals, are supposed to be closely related and interact with each other. Although the type of relationship between ENSO and IOD has not yet been fully demonstrated, extensive research has shown that both SST and the air-sea systems in the Pacific Ocean and the Indian Ocean are closely linked (Klein and Soden, 1999; Li et al., 2008; Huang and Kinter, 2002; Li et al., 2003; Annamalai et al., 2005; Cai et al., 2019). The Walker circulation anomaly induced by SSTA over the equatorial Pacific Ocean will cause a Walker circulation anomaly over the Indian Ocean, which could inspire the occurrence and development of IOD in the Indian Ocean driven by abnormal wind stress in the lower layer. On the other hand, Indonesian Throughflow also plays a role in the connection between ENSO and IOD. The cold (El Nino) or warm (La Nina) SST of the warm pool in the Pacific Ocean can cool or warm the SST in the eastern equatorial Indian Ocean through the Indonesian Throughflow, which is conducive to the establishment of a positive or negative phase of IOD.

Yang and Li (2005) found the first leading mode of the tropical Pacific-Indian SSTA reflecting the opposite phase characteristics of both the middle west Indian Ocean and equatorial middle east Pacific Ocean and both the eastern Indian Ocean and equatorial western Pacific Ocean, from which they proposed the concept of the Pacific-Indian Ocean associated mode (PIOAM), and noted that the PIOAM can better reflect the influence of the tropical SSTA on Asian atmospheric circulation. Yang et al. (2006) subsequently found that the influences of the PIOAM and the ENSO mode on summer precipitation and climate in China were very different, and their numerical experiments also showed that the simulation results obtained by considering the PIOAM were more consistent with observation data. Based on multi-variable empirical orthogonal functions, Chen and Cane (2008) and Chen (2011) also found this phenomenon and named it Indo-Pacific Tripole (IPT), which is considered to be an intrinsic mode in the tropical Indo-Pacific Ocean. In addition, Lian et al. (2014) used a conceptual model to discuss the development and physical mechanism of the IPT. By analyzing the monthly thermocline temperature anomaly (TOTA) from 1958-2007 and the weekly sea surface height (SSH) anomaly from 1992-2011 in the tropical Pacific–Indian Ocean, Li et al. (2013) further found that the PIOAM are more obviously in the subsurface ocean temperature anomaly field, especially in the thermocline. Based on the simulation results of the LASG/IAP (State Key Laboratory of Numerical Modeling for Atmospheric Sciences and Geophysical Fluid Dynamics/Institute of Atmospheric Physics) Climate system Ocean Model (LICOM), version 2 (LICOM2.0) (Liu et al. 2012) and observation data, Li and Li (2017) proved that PIOAM is an important tropical Pacific-Indian Ocean SST variation mode that actually exists both in observation and simulation. Therefore, when studying the influence of SSTA in the Pacific and Indian oceans on weather and climate, the Pacific and Indian oceans should be considered as unified.

Since the PIOAM is so important, how well do current climate models simulate it? To answer this question, the outputs from the climate system models for the Coupled Model Intercomparison Project (CMIP) phase 5 (CMIP5) were used for this research, from which we aim to provide a more complete evaluation of the PIOAM and try to find possible reasons that cause the simulation biases. In the following, Sect. 2 includes a brief description of the HadISST dataset, CMIP5 models, and the methods used in this study. Section 3 presents the assessments of the PIOAM in the CMIP5 models. A conclusion and discussion are given in Sect. 4.

2. Data and methods

The SST data from the Hadley Centre Global Sea Ice and Sea Surface Temperature (HadISST) (Rayner et al., 2003) dataset is used for this study. The data are monthly averaged data from 1951 to 2005 with a spatial resolution of 1°×1°. Brief information for the 21 CMIP5 models for the historical period used in this article is provided in Table 1. It's worth noting that some models have higher resolution in tropics. Considering that output data resolutions vary between the models, we first interpolated all data into a 1°×1° grid to facilitate comparison between the models and HadISST dataset.

Table 1. List of 21 selected CMIP5 climate models.

Model name	Modeling group	Oceanic resolution (lon×lat)
CanESM2 (Second Generation Canadian Earth System Model)	Canadian Centre for Climate Modeling and Analysis, Canada	256×192
CCSM4 (The Community Climate System Model, version 4)	NCAR, USA	320×384
CMCC-CESM (Centro Euro-Mediterraneo sui Cambiamenti Climatici (CMCC) Carbon Earth System Model)	CMCC, Italy	182×149
CMCC-CM (CMCC Climate Model)	CMCC, Italy	182×149
CMCC-CMS (CMCC-CM with a resolved stratosphere)	CMCC, Italy	182×149
CNRM-CM5 (Centre National de Recherches Météorologiques (CNRM) Coupled Global Climate Model, version 5)	CNRM, France	362×292
FGOALS-s2 (The Flexible Global Ocean-Atmosphere-Land System model, Spectral Version 2)	LASG, China	360×196
GFDL-ESM2M (Earth System Model of Geophysical Fluid Dynamics Laboratory (GFDL) with Modular Ocean Model, version 4)	GFDL, USA	144×90
GISS-E2-H (Goddard Institute for Space Studies (GISS) Model E version 2 (GISS-E2) with HYCOM ocean model)	NASA, USA	144×90
GISS-E2-H-CC (GISS-E2-H with carbon cycle)	NASA, USA	144×90
GISS-E2-R (GISS-E2 with Russell ocean model)	NASA, USA	144×90
GISS-E2-R-CC (GISS-E2-R with carbon cycle)	NASA, USA	144×90
HadCM3 (the third version of he Hadley Centre coupled model)	Met Office Hadley Centre, UK	288×144

HadGEM2-AO (Hadley Global Environment Model 2 (HadGEM2)-Atmosphere-Ocean)	Met Office Hadley Centre, UK	360×216
HadGEM2-CC (HadGEM2-Carbon Cycle)	Met Office Hadley Centre, UK	360×216
HadGEM2-ES (HadGEM2-Earth System)	Met Office Hadley Centre, UK	360×216
IPSL-CM5B-LR (Institut Pierre Simon Laplace Climate Model 5B (LPSL-CM5B)-Low Resolution)	IPSL, France	182×149
IPSL-CM5B-MR (LPSL-CM5B 5A-Medium Resolution)	IPSL, France	182×149
MIROC-ESM (Model for Interdisciplinary Research on Climate, Earth System Model)	Atmosphere and Ocean Research Institute (AORI), Japan	256×192
MIROC-ESM-CHEM (An atmospheric chemistry coupled version of MIROC-ESM)	AORI, Japan	256×192
NorESM1-M (Norwegian Climate Centre Earth System Model)	Norwegian Climate Centre, Norway	384×320

The PIOAM is determined according to the method of Ju et al. (2004) and Li et al. (2018), that is, the first leading mode (empirical orthogonal function, EOF1) of the tropical Pacific-Indian ocean SSTA (20°S-20°N, 40°E-80°W) is used to represent the PIOAM. The annual cycle and the linear trend are removed to obtain the monthly SSTA. Ju et al. (2004) used this method to analyze SSTA in the tropical Pacific-Indian Ocean in different seasons, and found the existence of PIOAM in all seasons with a contribution to total variance of more than 33%, indicating that the spatial distribution structure of PIOAM was stable.

Accounting for the intimate connection between the Pacific ENSO mode and the Indian Ocean dipole, Yang et al. (2006) argued that the PIOAM index (PIOAMI) can be defined as the respectively normalized east-west SSTA differences of the equatorial areas in the two oceans. As to the SSTA, the SSTA of ENSO is stronger than that in the equatorial Indian Ocean because of the larger Pacific basin; however, as to the influence of the SSTA on East Asia, a series of numerical experiments clearly indicate that the effect of SSTA forcing on the Indian Ocean is stronger than that of the eastern equatorial Pacific (Shen et al., 2001; Guo et al., 2002; Guo et al., 2004; Yang et al., 2006). Therefore, the PIOAMI is defined on the basis of the respective normalized dipoles in the Pacific and the Indian Ocean. According to the method of Yang et al. (2006), The PIOAMI is defined as follows:

$$\mathrm{PIOAMI} = \mathrm{IOI} + \mathrm{POI} \quad (1)$$

$$\mathrm{IOI} = \mathrm{SSTA}(5°\mathrm{S} - 10°\mathrm{N},\ 50°\mathrm{E} - 65°\mathrm{E}) - \mathrm{SSTA}(10°\mathrm{S} - 5°\mathrm{N}, 85°\mathrm{E} - 100°\mathrm{E}) \quad (2)$$

$$\mathrm{POI} = \mathrm{SSTA}(5°\mathrm{S} - 5°\mathrm{N},\ 130°\mathrm{W} - 80°\mathrm{W}) - \mathrm{SSTA}(5°\mathrm{S} - 10°\mathrm{N}, 140°\mathrm{E} - 160°\mathrm{E}) \quad (3)$$

where IOI and POI are the normalized Indian Ocean and Pacific Ocean indeices, respectively.

3. Results

3.1 Spatial pattern

Figure 1 shows the pattern of SST anomalies over the Indo-Pacific Ocean in October 1982 and September 1997. It can be clearly seen that there are obvious warm tongues in the eastern equatorial Pacific Ocean, obvious positive SST anomalies in the northwest Indian Ocean, and obvious negative SST anomalies in the western equatorial Pacific Ocean and the eastern Indian Ocean. This is precisely the typical spatial pattern characteristics of the PIOAM mentioned above. That is to say, the SST anomalies in the northwest Indian Ocean and the equatorial middle-east Pacific Ocean is opposite to the SST anomalies in the western equatorial Pacific Ocean and the east Indian Ocean. Compared with ENSO and IOD, the PIOAM has a broader spatial distribution.

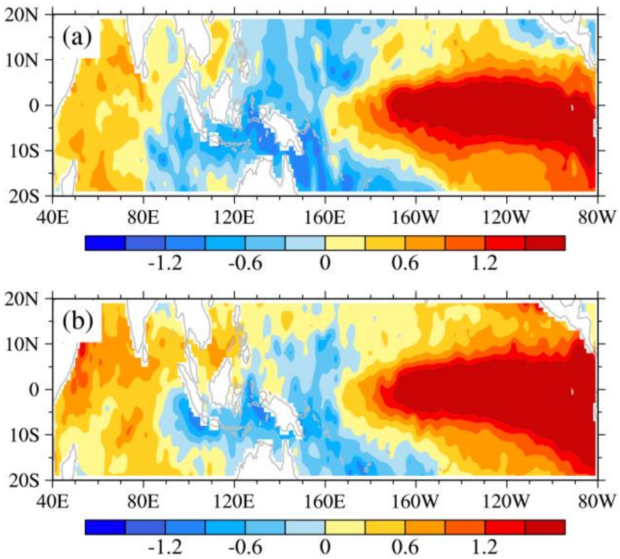

Figure 1: Maps of SST anomalies for (a) October 1982 and (b) September 1997 from the HadISST dataset (unit: °C). The period from 1981 to 2005 is used to extract the monthly SST climatology.

However, is this spatial pattern of SST anomalies only a special case of a certain year, or is it stable? To answer this question, EOF analysis is performed on the SST anomalies of different seasons over Indo-Pacific Ocean (20°S-20°N, 40°E-80W°) from 1951 to 2005. All these first leading modes in Fig. 2 are well separated from the remaining leading modes, based on the criteria of North et al. (1982), which means less likely to be affected by statistical sampling errors. It can be found that the patterns of summer (June, July and August; Fig. 2.b) and autumn (September, October and November; Fig. 2.c) display the typical spatial distribution of the PIOAM, with the 46% and 61% contribution to total variance, respectively, while the spatial pattern of PIOAM is not so obvious in spring (March, April and May; Fig. 2.a) and winter (December, January and February; Fig. 2.d). In general, the PIOAM has stable structure and practical significance, especially in autumn.

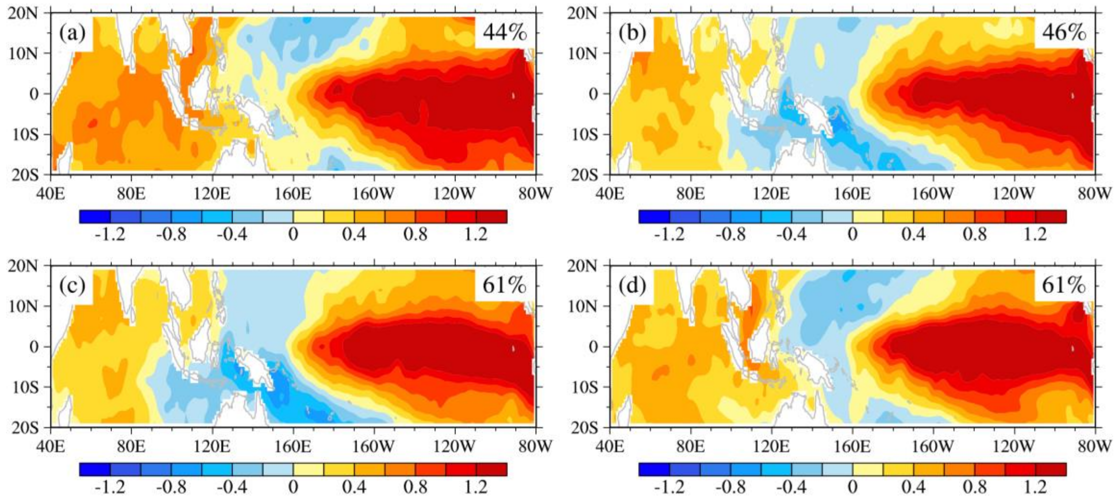

Figure 2: Spatial patterns of the first leading mode of the (a) spring (March, April and May), (b) summer (June, July and August), (c) autumn (September, October and November) and (d) winter (December, January and February) averaged SST anomalies over Indo-Pacific Ocean (20°S-20°N, 40°E-80W°) calculated from HadISST dataset (unit: °C). The numbers at the upper right corner of each panel indicate the percentage of variance explained by each season.

Performing the EOF analysis on the monthly SST anomalies regardless of seasonal differences, Figure 3 depicts the spatial pattern of PIOAM in the selected 21 CMIP5 models and their differences compared to HadISST dataset (Fig. 3a). Figure 3.b shows the results of a multi-model ensemble (MME) that represents the mean of the results from all selected models. The PIOAM in HadISST dataset and CMIP5 models is well separated from the second leading mode, according to the criterion of North et al. (1982). To better and objectively evaluate the capability of each model in simulating PIOAM, a Taylor diagram (Fig. 4) is also adopted to concisely display the relative information from multiple models, so that the differences among the simulations from all models are revealed clearly (Taylor, 2001; Jiang and Tian, 2013; Yang et al., 2018). According to HadISST dataset (Fig. 3.a), with a 47% contribution to total variance, the PIOAM has a warm tongue spatial pattern in the eastern equatorial Pacific Ocean, whereas there is negative SSTA in the western equatorial Pacific Ocean, which exhibits an obvious ENSO mode in the Pacific Ocean. In addition, there are obvious positive SSTA in the western Indian Ocean region of the PIOAM, but the SSTA in the eastern equatorial Indian Ocean region remain positive. Considering that the ~~so-called~~ IOD is defined by the difference between the SSTA in the western equatorial Indian Ocean and that in the eastern equatorial Indian Ocean, this indicates zonal surface heat contrast of the Indian Ocean SSTA. Although it is called a dipole, it is also like a meridional seesaw ~~not related to the mathematic meaning~~ (Li et al., 2002; Yang et al., 2006). Therefore, it can be considered that the PIOAM represents an IOD mode in the Indian Ocean region.

Figure 3 shows that all of these models can generally reproduce the spatial pattern of PIOAM, yet large discrepancies exist regarding the strength, and the differences between the models are also significant. Except for the contribution to total variance of PIOAM in CCSM4 and CMCC-CESM are nearly consistent with HadISST dataset, the variance contribution of PIOAM in almost all CMIP5 models are lower than those in the HadISST dataset, especially CMCC-CM with a contribution to total variance as small as 26%. In terms of strength, it is apparent that the simulation errors of these models are mainly concentrated in the Pacific Ocean compared to the Indian Ocean. Compared to the HadISST dataset, a majority of models overestimate the strength of PIOAM in the equatorial east Pacific and central Pacific; only one-seventh of the models (IPSL-CM5A-LR, IPSL-CM5A-MR and MIROC-ESM) underestimate the strength of PIOAM in the equatorial east Pacific, while the simulation results of HadGEM2-AO and CMCC-CM in the equatorial central Pacific and western Pacific are weak. The simulation errors of the strength of the ENSO-like mode in CCSM4, CMCC-CMS, GFDL-ESM2M and GISS-E2-R-CC are lower than those in other models. For the Indian Ocean, the strengths of PIOAM in only approximately one-quarter of the models (CanESM2, CMCC-CESM, GISS-E2-H-CC, HadCM3 and HadGEM2-AO) are basically consistent with HadISST dataset with small simulation errors. Nearly half of the models were smaller for the eastern Indian Ocean, whereas more than half were larger for the western Indian Ocean. In general, the simulation error in the Indian Ocean region is significantly smaller than that in the Pacific region. According to Fig. 4, it is apparent that the root mean square errors (RMSEs) in MIROC-ESM-CHEM, IPSL-CM5A-LR and MIROC-ESM are relatively large, which means that the capabilities of these modes to simulate the strength of PIOAM are still inadequate, whereas the RMSEs in CCSM4, CMCC-CMS and GFDL-ESM2M are smaller than in other models with a better performance. In addition, as shown in Fig. 3.b, MME better simulates the amplitude of PIOAM in the Indian Ocean than most these selected CMIP5 models with smaller simulation errors, but the amplitude in the equatorial Pacific are larger than that of the HadISST dataset.

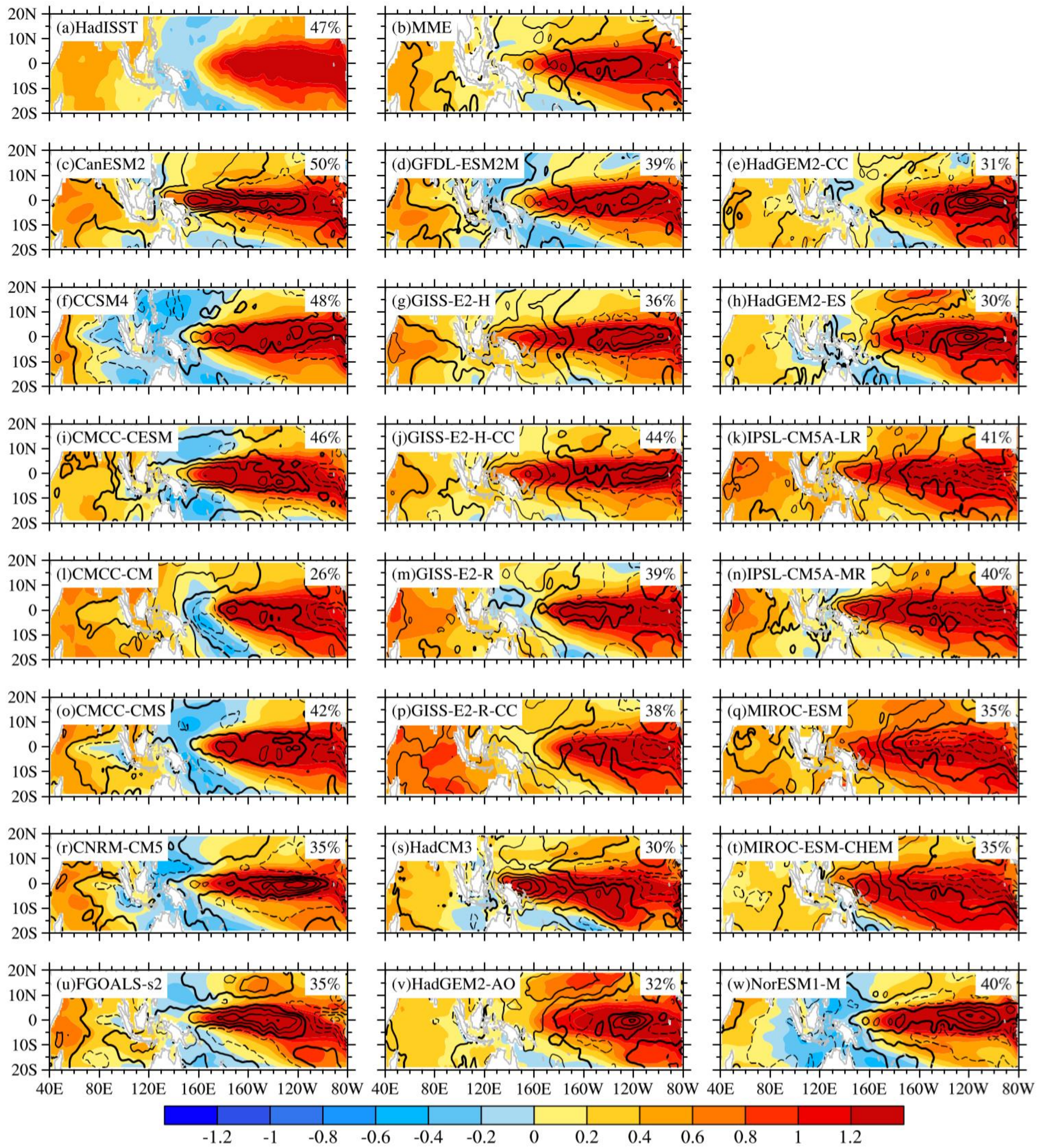

Figure 3: PIOAM (shading) and the difference between each model and HadISST dataset (contour, with an interval of 0.3, shown as black bold lines represent the contour with the zero value, dashed contours denote negative values, unit: °C). The numbers at the upper right corner of each panel indicate the percentage of variance explained by each model.

As for spatial patterns, the IOD-like mode in the Indian Ocean region can be simulated in almost all models except MIROC-ESM-CHEM. Although all these models reproduce the spatial pattern of the positive SSTA well in the eastern equatorial Pacific, only one-third of the models (CCSM4, CMCC-CM, CMCC-CMS, CNRM-CM5, FGOALS-s2, GFDL-ESM2M and NorESM1-M) successfully simulate the ENSO-like mode with the east-west inverse phase in the Pacific Ocean. In addition, the simulated positive SSTAs in the eastern equatorial Pacific in HadCM3 and MIROC-ESM-CHEM are further south. According to Fig. 4, more than one-third of these models (CCSM4, CMCC-CMS and GFDL-ESM2M, etc.) can simulate the spatial pattern of PIOAM well, and the spatial correlation coefficients between these models and the HadISST dataset are all greater than 0.9, especially CCSM4, which is as high as 0.95. In contrast, the spatial pattern of PIOAM in MIROC-ESM-CHEM is unsatisfactory with a spatial correlation coefficient of only 0.69. The simulation results of HadCM3 and MIROC-ESM are also relatively poor, and the spatial correlation coefficients with HadISST dataset are less than 0.8. It can also be learned from Fig. 4 that, for the standard deviation of PIOAM, very large differences exist among these models. The standard deviations of PIOAM in IPSL-CM5A-LR, MIROC-ESM and GISS-E2-R-CC are quite different from those of the HadISST dataset, while the simulation results of CMCC-CMS, GFDL-ESM2M and HadGEM2-CC are basically close to those of the HadISST dataset and have better performance. It is noteworthy that the standard deviations of PIOAM in more than half of these models are smaller than that of the HadISST dataset, and their differences are large. Although the spatial pattern of PIOAM in MME is closer to the HadISST dataset and the RMSE is smaller than the vast majority of single models, the standard deviation of PIOAM in MME is smaller than that of the HadISST dataset.

In general, CCSM4, GFDL-ESM2M and CMCC-CMS have a stronger ability to simulate the PIOAM. In addition, although the MME ~~of these models~~ may not be as good as that of a single model in some specific aspects, overall, considering spatial pattern, standard deviation and RMSE, MME is still superior to most single models.

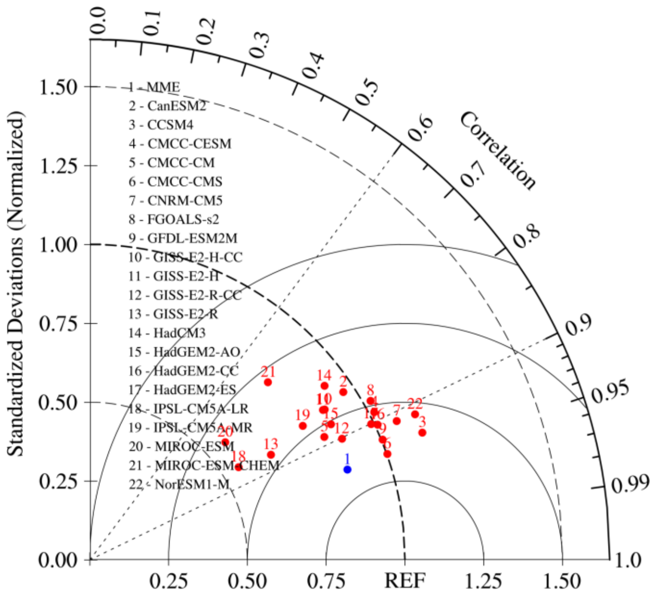

Figure 4: Taylor diagram of PIOAM.

To further evaluate the differences between these models, Fig. 5 shows the distribution of standard deviations between the CMIP5 models, which clearly reflects the regional differences between the models. It is apparent that the differences are mainly concentrated in the eastern equatorial Pacific. Therefore, the emphasis of improving the model on simulating the PIOAM is to improve the capability of the model to simulate to the Eastern-Pacific (EP) type ENSO.

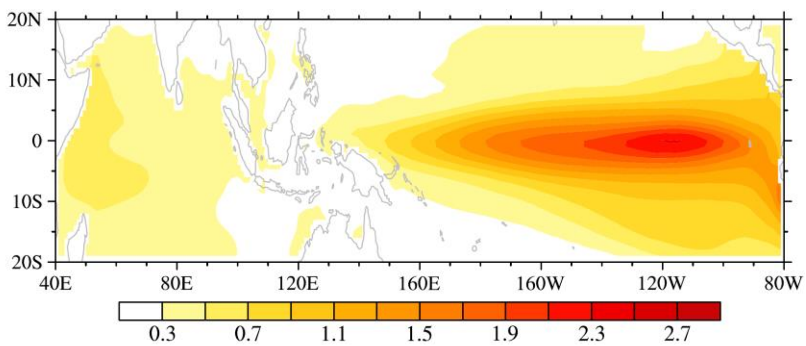

Figure 5: The standard deviations of simulated PIOAM between the selected 21 CMIP5 models (unit: °C).

3.2 PIOAM index

3.2.1 Time series

A satisfactory index is needed to describe the PIOAM. It is customary to select the time coefficient (PC1) of the PIOAM as its index. It can be seen from the regression of the monthly SSTA onto the normalized PC1 (Fig. 6.a) that the pattern in the Pacific Ocean is similar to ENSO, but positive SST anomalies occur throughout the Indian Ocean, which not matches the typical PIOAM spatial pattern. This is because the ENSO signals in the Pacific Ocean in PC1 are so strong that the signals of the IOD are not fully reflected. The correlation coefficient between PC1 and Niño3.4 index is as high as 0.95. However, obvious negative SST anomalies in the eastern Indian Ocean can be found in the regression map of the monthly SSTA based on the normalized PIOAMI defined in Section 2. The correlation coefficient between PIOAMI and Niño3.4 index is 0.68, indicating PIOAMI contains more Indian Ocean signals than PC1. In addition, the correlation coefficient between PC1 and PIOAMI is 0.70, which is far more than the confidence level of 99%. Therefore, PIOAMI can describe the mode well because of giving consideration to both the signals in the Pacific Ocean and the signals in the Indian Ocean.

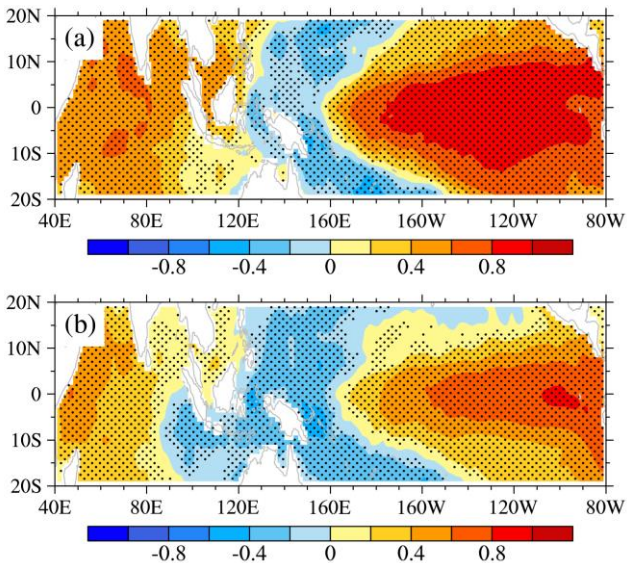

Figure 6: Regressions of the monthly SSTA onto the normalized (a) PC1 and (b) PIOAMI for the period from 1951 to 2005 (unit: °C). The stippled areas for SSTA denote the 99% confidence levels.

Figure 7. shows the monthly time series of the PIOAMI, Pacific Ocean index (POI) and Indian Ocean index (IOI) from 1951 to 2005. The wavelet analysis of PIOAMI indicates that PIOAM has obvious seasonal and interannual variations, as well as interdecadal variations (feature is omitted). According to Fig. 7, POI and IOI have the same variation tendency at most times, thus the PIOAMI amplitude is greatly enhanced. However, there are a few cases where the two change in opposing ways, resulting in a much weaker PIOAMI. Moreover, from the time-series of PIOAMI, there is an interannual

oscillation of positive and negative phases in the PIOAM, and there is also a phenomenon that the PIOAMI is very weak or not obvious in some years.

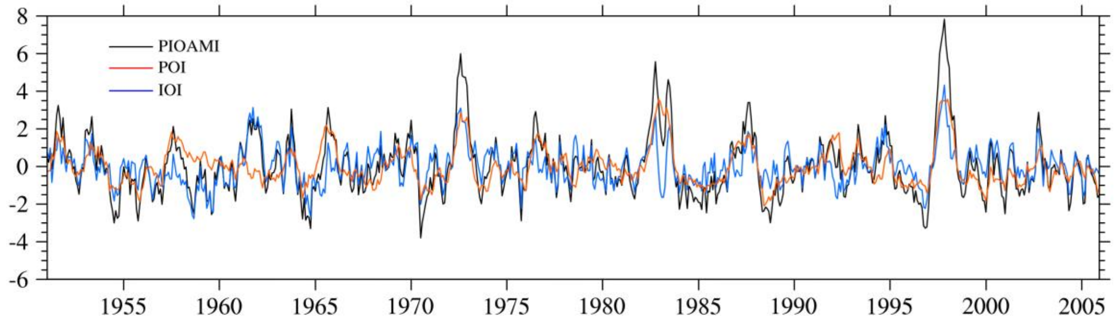

Figure 7: Time-series of PIOAM index (black), Pacific Ocean index (red) and Indian Ocean index (blue) in the HadISST dataset.

Considering that the PIOAM mainly reaches its peak in autumn (September, October and November), we select the year with significant positive and negative phases of PIOAM by taking one standard deviation as the criterion, and calculate the difference of autumn PIOAMI between each CMIP5 model and the HadISST dataset (see Fig. 8) to further reveal the simulation of the CMIP5 models on the strength of the PIOAM. As shown by Fig. 8.a, the simulated strengths of the PIOAM in the positive phase are underestimated in most models, whereas they are slightly overestimated in less than one-fifth of the models (CCSM4, CMCC-CMS, CNRM-CM5 and GFDL-ESM2M) are slightly stronger, which are very close to the HadISST dataset, especially in CCSM4. However, nearly half of the models overestimate the strength of the PIOAM in the negative phase (Fig. 8.b), in which the simulation results of CanESM2 and GISS-E2-R are consistent with the HadISST dataset. Although CCSM4 has a better performance in simulating the strength of the PIOAM in the positive phase than other models, the simulation error of the negative phase is very large.

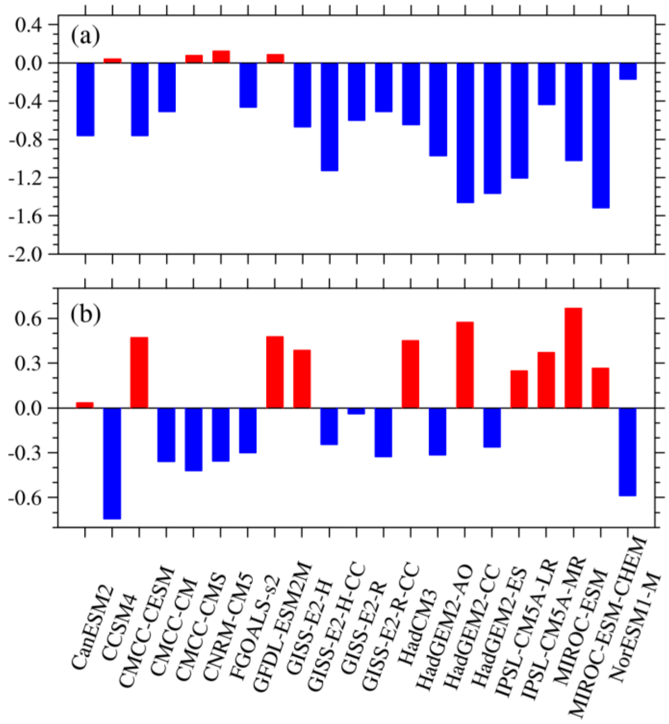

Figure 8: Difference in the amplitude of the PIOAMI in the positive phase (a) and negative phase (b) between the CMIP5 models and HadISST dataset.

According to PIOAM positive and negative phase year based on the autumn PIOAMI, SSTAs in the tropical Pacific-Indian Ocean in October are composited to obtain the spatial pattern of SSTAs in the PIOAM positive and negative phases. It is clear in Fig. 9 that the SSTAs in the Pacific-Indian Ocean in both the MME of CMIP5 models and HadISST dataset present patterns with a tripole structure, where the Indian Ocean is represented by the IOD-like mode and the Pacific Ocean by the ENSO-like mode, which again demonstrates the authenticity of PIOAM and the rationality of PIOAMI used in this article.

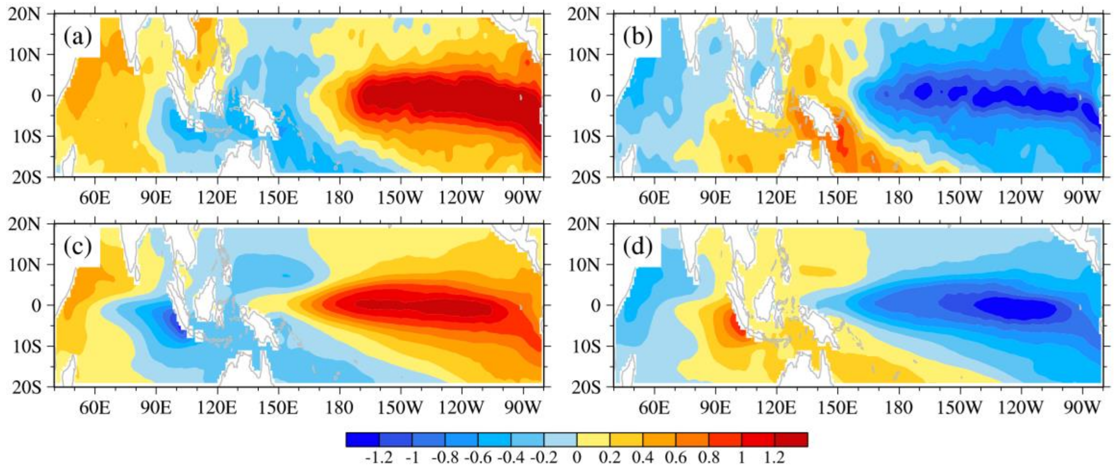

Figure 9: The tropical Pacific-Indian Ocean SSTAs of the PIOAM positive (a, c) and negative (b, d) phase in

October in the HadISST dataset (a, b) and the MME of CMIP5 models (c, d) (unit: °C).

3.2.2 Interannual Variation of PIOAM

To evaluate the ability of these CMIP5 models to simulate the interannual variation of PIOAM, Fig. 10 shows the ratios of standard deviation of IOI, POI and PIOAMI in autumn in each model to those in the HadISST dataset. The closer the ratio is to 1, the better the ability to simulate interannual variation. It can be found that the difference in the simulation results of the interannual variation of PIOAMI among these models is smaller compared to IOI and POI. The simulation results of CCSM4, GISS-E2-R and FGOALS-s2 are almost consistent with HadISST dataset, indicating that these three models have relatively strong capabilities to simulate the interannual variation of PIOAM. Except that NorESM1-M overestimates the interannual variation of PIOAM, the simulation results in most of the models are weak, especially MIROC-ESM, which leads to MME underestimating the interannual variation of PIOAM compared to the HadISST dataset. In addition, the interannual variations of IOI in GFDL-ESM2M, GISS-E2-R-CC and CMCC-CM are better than other models, whereas the simulation results are underestimated in most models. In contrast to IOI, the vast majority of models overestimate the interannual variations of POI, and the simulated interannual variations of POI in only three models (IPSL-CM5A-MR, CMCC-CESM and IPSL-CM5A-LR) are weaker than the HadISST dataset. Based on the above analysis, it is apparent that the interannual variation of PIOAMI is more closely to IOI than POI, and the interannual variation of PIOAM in autumn can be measured by CCSM4, GISS-E2-R and FGOALS-s2.

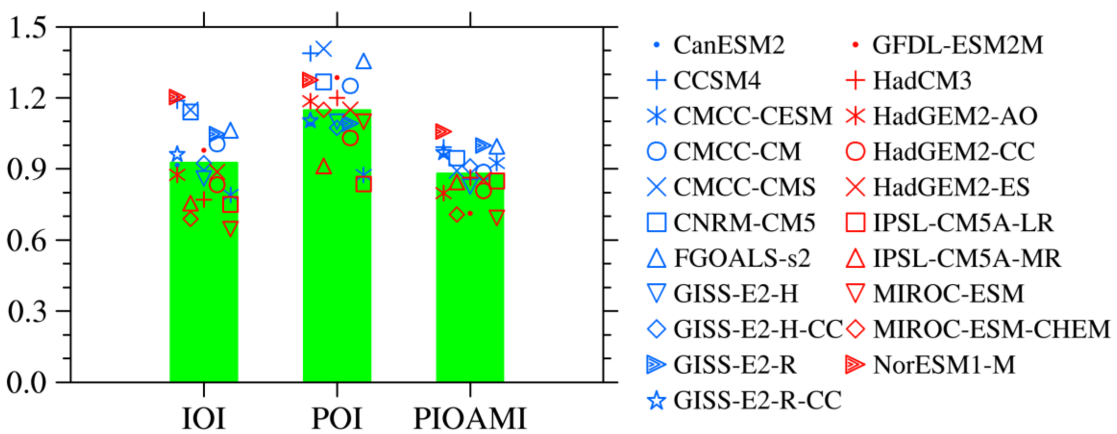

Figure 10: Ratios of standard deviation of autumn IOI, POI and PIOAMI in each model to those in the HadISST dataset. Green bar represents the MME of the corresponding index.

3.2.3 The relationship of PIOAM with ENSO and IOD

The lag-lead correlation analysis between PIOAMI and the Niño3.4 index derived from the HadISST dataset shows that PIOAM has a close correlation with the ENSO mode at the same period and one month lagging with the correlation coefficient of 0.68 (Fig. 11.a). In addition, PIOAM and IOD also have a close correlation in the same period, with a correlation coefficient of 0.73 (Fig. 11.b), indicating that the PIOAM can reflect the activities of ENSO in the Pacific Ocean and IOD in the Indian Ocean to a considerable extent. It should be noted that the IOD index used in this research is according to the definition of Saji et al. (1999), i.e. the difference in SSTA between the tropical western Indian Ocean (50°E-70°E, 10°S-10°N) and the tropical south-eastern Indian Ocean (90°E-110°E, 10°S-0). In these CMIP5 models, more than one-half of the models successfully reproduce the maximum correlation between PIOAM and ENSO in the same period. The correlation coefficients of the PIOAMI and the Niño3.4 index in HadGEM2-AO and HadGEM2-ES are both 0.68, which is consistent with the HadISST dataset, and the correlation coefficients of FGOALS-s2, GISS-E2-H and GISS-E2-H-CC are 0.69, 0.69 and 0.70, respectively. However, the correlation coefficients of MIROC-ESM and MIROC-ESM-CHEM are only 0.37 and 0.30, which are significantly different from the results of the HadISST dataset and other models, indicating that the two models cannot simulate the close relationship between the PIOAM and ENSO well. In addition, the correlation coefficient of PIOAMI and the Niño3.4 index in MME is 0.66, which is slightly lower than the HadISST dataset but shows the close contemporaneity correlation between the PIOAM and ENSO; the overall change of the correlation coefficient series is very close to the HadISST dataset.

For the relationship between the PIOAM and IOD, it is apparent from the HadISST dataset in Fig. 11.b that the PIOAM and IOD show obvious close correlation in the same period, and the correlation coefficient is as high as 0.73. It is satisfactory that all selected CMIP5 models successfully reproduce the correlation between PIOAM and IOD in the same period, but the simulation results in more than half of them are underestimated. Among these models, the simulation results of HadGEM2-ES and GIS-E2-R-CC are basically consistent with the HadISST dataset, which shows that the two models have stronger capability to simulate the relationship between PIOAM and IOD.

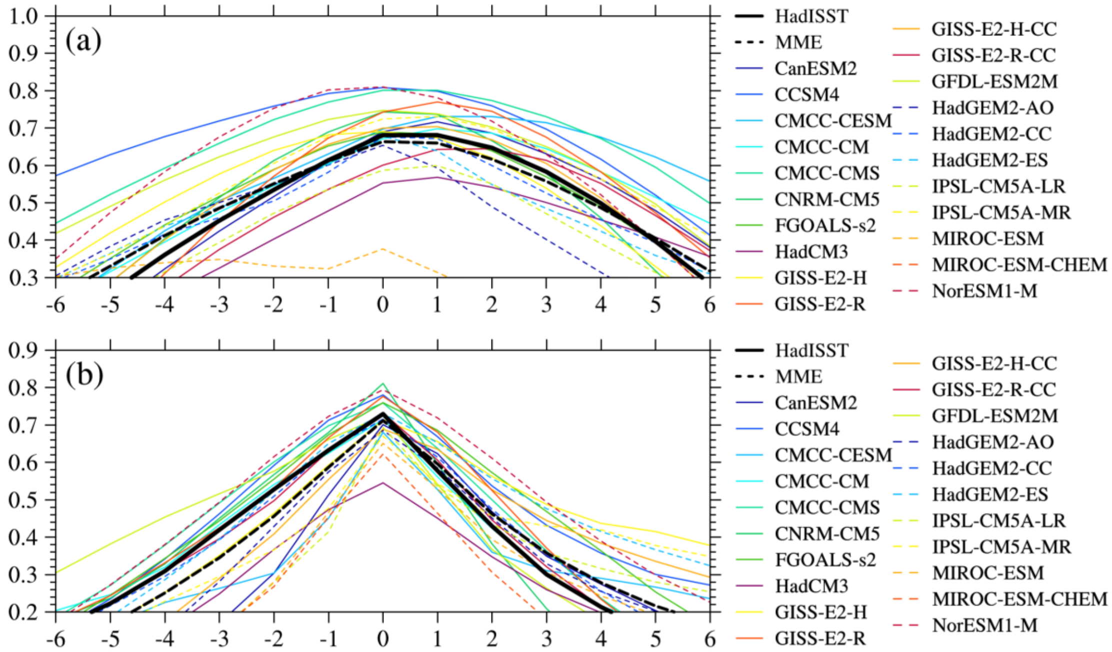

Figure 11: The lag-lead correlation coefficient of the PIOAMI with the Niño3.4 index (a) and IOD index (b). Ordinate represents the correlation coefficient, and abscissa is the lag in months: positive (negative) for the Niño3.4 index or IOD index (PIOAMI) leading PIOAMI (Niño3.4 index or IOD index)

~~4. Possible causes of simulation errors~~

~~It is undoubtedly difficult to directly find the factors that influence the model to simulate the PIOAM. However, the simulation results of model families, such as CMCC, IPSL, MIROC, GISS and HadGEM2, provide comparative data to find the possible reasons that may lead to simulation differences. Using the CMCC model family as an example, CMCC-CM is a climate model. Because of this, CMCC-CM, CMCC-CESM and CMCC-CMS consider more complete physical processes and closer to the real world. CMCC-CESM is a carbon earth system model, and CMCC-CMS is a climate model with a resolved stratosphere. It can be found from Fig. 3.i, l and o that although CMCC-CM, CMCC-CESM and CMCC-CMS all overestimate the strength of the PIOAM in the equatorial eastern Pacific Ocean, CMCC-CESM also overestimates it in western Pacific Ocean, but CMCC-CM is weak. While the simulation results in CMCC-CMS in the Pacific Ocean, especially the equatorial western Pacific Ocean, are better than that in CMCC-CM and CMCC-CESM, but the strength of the PIOAM in the East Indian Ocean is weak in CMCC-CMS. In addition, the variance contribution of PIOAM in CMCC-CESM is very close to that in the HadISST dataset, reaching 46%, followed by CMCC-CMS with 42%, while CMCC-CM only has 26%. As shown in Fig. 4, not only is the spatial pattern of PIOAM in CMCC-CMS better with a higher spatial correlation coefficient, the RMSE is smaller and the standard deviation of PIOAM is basically~~

consistent with the HadISST dataset. It can be found that considering the carbon cycle or resolving the stratosphere can effectively improve the capability to simulate the PIOAM.

Moreover, from the simulation results of GISS-E2-H and GISS-E2-H-CC, it can also be found that after considering the carbon cycle, GISS-E2-H-CC has no obvious improvement concerning the spatial pattern of PIOAM, and the RMSEs in GISS-E2-H and GISS-E2-H-CC are basically the same. However, the variance contribution of PIOAM in GISS-E2-H-CC is significantly improved compared to that in GISS-E2-H, ranging from 36% to 44%, which is closer to the HadISST dataset. Unlike GISS-E2-H and GISS-E2-H-CC, the variance contributions of PIOAM in GISS-E2-R and GISS-E2-R-CC are almost the same, but with a smaller RMSE, the spatial pattern and standard deviation of PIOAM in GISS-E2-R-CC are more consistent with the HadISST dataset than that in GISS-E2-R (see Fig. 4). Furthermore, in the HadGEM2 model family, HadGEM2-CC considers the carbon cycle on the basis of HadGEM2-AO. Compared to HadGEM2-AO, the RMSE of HadGEM2-CC is smaller, and the spatial type and standard deviation of PIOAM are more consistent with the HadISST dataset. Again, the performance of HadGEM2-CC effectively verifies the importance of the carbon cycle.

A comparison of the performance of MIROC-ESM and MIROC-ESM-CHEM revealed that the chemical process also has an obvious influence on the simulation results of PIOAM. After the chemical process is accounted for, the spatial standard deviation of PIOAM in MIROC-ESM-CHEM is closer to the HadISST dataset than that in MIROC-ESM, but the RMSE in MIROC-ESM-CHEM is slightly larger. The same is true for HadGEM2-E and HadGEM2-CC, indicating that the chemical process can effectively improve the simulation effect of the standard deviation of PIOAM.

In addition, it can be found from the two models from the IPSL-CM5A family (IPSL-CM5A-LR with low atmospheric resolution 95×96 and IPSL-CM5A-MR with medium atmospheric resolution 143×144) that atmospheric resolution also affects the PIOAM simulation results. The RMSE in IPSL-CM5A-MR is slightly smaller than that in IPSL-CM5A-LR, and the spatial pattern of PIOAM is slightly better. Moreover, the simulated standard deviation of PIOAM in IPSL-CM5A-MR is much closer to the HadISST dataset than that in IPSL-CM5A-LR. This indicates that reasonably increasing the horizontal resolution of atmospheric model may also improve the simulation effect on PIOAM.

4. Conclusion and discussion

Based on HadISST dataset from 1951 to 2005, the Pacific-Indian Ocean associated mode, proposed by Yang and Li (2005) is evaluated for 21 CMIP5 models. This research provides a relatively comprehensive evaluation of the spatial pattern, the interannual variation and the relationship with ENSO and IOD of the PIOAM in the selected CMIP5 models. The main conclusions are as follows.

With a 47% contribution to total variance, the spatial pattern of PIOAM in the eastern equatorial Pacific Ocean is a warm tongue, whereas there is negative SSTA in the western equatorial Pacific Ocean that exhibits an obvious ENSO mode in the Pacific Ocean. In addition, the PIOAM presents an IOD mode in the Indian Ocean. The variance contributions of PIOAM in almost all CMIP5 models are smaller than that in the HadISST dataset. The simulation errors and differences among these models are mainly concentrated in the Pacific Ocean, compared to the Indian Ocean, and a majority of models overestimate the strength of PIOAM in the equatorial east Pacific and central Pacific. Although all these models reproduce the spatial pattern of the positive SSTA in the eastern equatorial Pacific well, only one-third of the models (CCSM4, CMCC-CM, CMCC-CMS, CNRM-CM5, FGOALS-s2, GFDL-ESM2M and NorESM1-M) successfully simulate the ENSO mode with the east-west inverse phase in the Pacific Ocean. In general, CCSM4, GFDL-ESM2M and CMCC-CMS have stronger capability to simulate the PIOAM than the other models.

The PIOAM is very weak or not obvious in some years and has obvious seasonal and interannual variations, as well as interdecadal variations. The simulated strengths of the PIOAM in the positive phase are underestimated in most models; only less than one-fifth of the models (CCSM4, CMCC-CMS, CNRM-CM5 and GFDL-ESM2M) are slightly stronger, and very close to the HadISST dataset, especially CCSM4. The interannual variation of PIOAM in CCSM4, GISS-E2-R and FGOALS-s2 are almost consistent with the HadISST dataset. Except that NorESM1-M overestimate the interannual variation of PIOAM, the simulation results in most models are weak, especially MIROC-ESM. The interannual variation of PIOAM in autumn can be measured by CCSM4, GISS-E2-R and FGOALS-s2. The PIOAM can well reflect the activities of ENSO in the Pacific Ocean and IOD in the Indian Ocean to a considerable extent with a close correlation to ENSO and IOD for the same period, as well as one month in advance with ENSO.

~~Considering the carbon cycle or resolving the stratosphere can effectively improve the capability of the model to simulate the PIOAM, a comparison of the performance of MIROC-ESM and MIROC-ESM-~~

~~CHEM revealed that the chemical process also has an obvious influence on the simulation results of PIOAM. The chemical process can effectively improve the simulation effect of the standard deviation of PIOAM. In addition, increasing the horizontal resolution of atmospheric model may improve the simulation effect on PIOAM as well.~~

It is undoubtedly difficult to directly find the factors that influence the model to simulate the PIOAM. The simulation results of model families, such as CMCC, IPSL, MIROC, GISS and HadGEM2, provide clues and comparative data to find the possible reasons that may lead to simulation differences. However, it needs in-depth analysis which is supported by a large number of models, or by dedicated experiments.

Yang et al. (2006) found that only considering the ENSO in the Pacific cannot entirely explain the influence of SSTA on climate variation, and suggested that, to provide better scientific explanation for short-term climate prediction, the PIOAM and its influence should be considered and investigated. In addition, a review article by Cai et al. (2019) provides the first comprehensive review and summary of the current research advances in the interaction between the tropical Pacific-Indo-Atlantic climate systems, and they pointed out that an in-depth understanding of the dynamic mechanisms of intertropical basin interactions is an important way to improve the ability of seasonal to decadal climate prediction. Therefore, evaluating and improving the capability of current climate models to simulate the PIOAM and even the tropical Pacific-Indo-Atlantic climate systems are beneficial to obtain accurate climate change predictions. In addition, improving the level of climate prediction is not only helpful to grasp the changes in the ocean environment of the Pacific-Indian Ocean, but also propitious to improve the ability of prediction and assessment of ocean waves and wind energy (Zheng and Li, 2015; Zheng and Li, 2017).

Data availability. The CMIP5 data are available at https://esgf-node.llnl.gov/search/cmip5/. The sea surface temperature are available at https://www.metoffice.gov.uk/hadobs/hadisst/data/download.html

Author contributions. Xin Li and Weilai Shi conceived the idea and designed the structure of this paper; Minghao Yang performed the experiments; Minghao Yang, Chao Zhang and Jianqi Zhang analyzed the data; Minghao Yang wrote the paper.

Competing interests. The author declares that they have no conflict of interest.

Author Contributions. This research was supported by National Natural Science Foundation of China (4160501, 41490642, 41520104008).

References:

Annamalai, H., Xie, S. P., Mccreary, J. P. and Murtugudde, R.: Impact of Indian Ocean Sea Surface Temperature on Developing El Niño. J. Clim., 18(1), 302-319, doi:10.1175/jcli-3268.1, 2005.

Bjerknes, J.: A possible response of the atmospheric Hadley circulation to equatorial anomalies of ocean temperature, Tellus., 18(4), 820-829, doi:10.3402/tellusa.v18i4.9712, 1966.

Bjerknes, J.: Atmospheric teleconnections from the equatodal Pacific, Mon. Wea. Rev., 97(3), 163-172, doi:10.1175/1520-0493(1969)097<0163:atftep>2.3.co;2, 1969.

Cai, W. J., Hendon, H. H. and Meyers, G.: Indian Ocean dipolelike variability in the CSIRO Mark 3 coupled climate model, J. Climate, 18(10), 1449-1468, doi: 10.1175/jcli3332.1, 2005.

Chen, D., Cane, M. A.: El Niño prediction and predictability, J. Comput. Phys., 227, 3625-3640, doi: 10.1016/j.jcp.2007.05.014, 2008.

Chen, D.: Indo-Pacific Tripole: An intrinsic mode of tropical climate variability, Adv. Geosci., 24, 1-18, doi: 10.1142/9789814355353_0001, 2011.

Cai, W., Wu, L., Lengaigne, M., Li, T., McGregor, Shayne., and et al.: Pantropical climate interactions, Science, 363(eaav4236), doi: 10.1126/science.aav4236, 2019.

Guo, Y. F., Zhao, Y. and Wang, J.: Numerical simulation of the relationships between the 1998 Yangtze River valley floods and SST anomalies, Adv Atmos Sci, 19(3), 391-404, doi:10.1007/s00376-002-0074-0, 2002.

Guo, Y. F.: Numerical simulation of the 1999 Yangtze River valley heavy rainfall including sensitivity experiments with different anomalies, Adv Atmos Sci, 19(3), 391-404, doi: 10.1007/BF02915677, 2004.

Huang, B. H. and Kinter, J. L.: Interannual variability in the tropical Indian Ocean, J. Geophys. Res., 107(C11): 3199. doi:10.1029/2001JC001278, 2002.

Jin, F. F.: An equatorial ocean recharge paradigm for ENSO. Part I: Conceptual model, J. Atmos. Sci., 54(7), 811-829, doi:10.1175/1520-0469(1997)054<0811:aeorpf>2.0.co;2, 1997.

Ju, J. H., Chen, L. L. and Li, C. Y.: The preliminary research of Pacific-Indian Ocean sea surface tempertature anomaly mode and the definition of its index, Journal of Tropical Meteorology (in chinese), 20(6), 617-624, 2004.

Jiang, D. B. and Tian, Z. P.: East Asian monsoon change for the 21st century: results of CMIP3 and CMIP5 models, Chinese Science Bulletin, 58(12), 1427-1435, doi:10.1007/s11434-012-5533-0, 2012.

Klein, S. A. and Soden, B. J.: Remote sea surface temperature variation during ENSO: evidence for a tropical atmospheric bridge, J. Clim., 12(4), 917-932, doi:10.1175/1520-0442(1999)012<0917:rsstvd>2.0.co;2, 1999.

Li, C. Y. Interaction between anomalous winter monsoon in East Asia and El Niño events, Adv. Atmos. Sci., 7(1), 36-46, doi:10.1007/bf02919166, 1990.

Li, C. Y. and Mu, M. Q.: El Niño occurrence and sub-surface ocean temperature anomalies in the Pacific warm pool, Chinese Journal of Atmospheric Sciences (in Chinese), 23(5), 513-521, 1999.

Li, C. Y. and Mu, M. Q.: Relationship between East Asian winter monsoon, warm pool situation and ENSO cycle, Chin. Sci. Bull., 45(16), 1448-1455, doi:10.1007/BF02898885, 2000.

Li, C. Y. and Mu, M. Q.: The influence of the Indian Ocean dipole on atmospheric circulation and climate. Adv. Atmos. Sci., 18(5), 831-843. doi:10.1007/BF03403506, 2001.

Li, C. Y.: A Further Study of the Essence of ENSO, Climate and Environmental Research (in Chinese), 7(2), 160-174, 2002.

Li, C. Y., Mu, M. Q., and Pan, J.: Indian Ocean temperature dipole and SSTA in the equatorial Pacific Ocean, Chin. Sci. Bull., 47(3), 236-239, doi:10.1360/02tb9056, 2002.

Li, T., Wang, B., Chang, C. P. and Zhang, Y.: A theory for the Indian Ocean dipole-zonal mode, J. Atmos. Sci., 60(17): 2119-2135, doi: 10.1175/1520-0469(2003)060<2119:atftio>2.0.co;2, 2003.

Li, C. Y., Mu, M., Zhou, G. Q. and Yang, H.: Mechanism and prediction studies of the ENSO, Chinese Journal of Atmospheric Sciences (in Chinese), 32(4), 761-781, 2008.

Liu, H., Lin, P., Yu, Y. and Zhang, X.: The baseline evaluation of LASG/IAP Climate system Ocean Model (LICOM) version 2, Acta. Meteor. Sin., 26(3), 318-329, doi:10.1007/s13351-012-0305-y, 2012.

Lian, T., Chen, D. K., Tang, Y. M., Jin, B. G.: A theoretical investigation of the tropical Indo-Pacific tripole mode, Sci. China-Earth Sci., 57, 174-188, doi: 10.1007/s11430-013-4762-7, 2014.

Li, X. and Li, C. Y.: The tropical pacific–indian ocean associated mode simulated by licom2.0, Adv. Atmos. Sci., 34(12), 1426-1436, doi:10.1007/s00376-017-6176-5, 2017.

Li, C. Y., Li, X., Yang, H., Pan, J. and Li, G.: Tropical Pacific-Indian Ocean Associated Mode and Its Climatic Impacts Chinese Journal of Atmospheric Sciences (in Chinese), 42(3), 505-523, 2018.

Mu, M. and Duan, W. S.: A new approach to studying ENSO predictability: Conditional nonlinear optimal perturbation, Chin. Sci. Bull., 48(10), 1045-1047, doi:10.1007/BF03184224, 2003.

Mu, M., Duan, W. S. and Wang, B.: Season-dependent dynamics of nonlinear optimal error growth and El Niño-Southern Oscillation predictability in a theoretical model, Journal of Geophysical Research: Atmospheres, 112(D10), doi:10.1029/2005JD006981, 2007.

North G. R., Bell, T. L., Cahalan, R. F., Moeng, F. J.: Sampling errors in the estimation of empirical orthogonal functions, Mon. Wea. Rev., 110, 699-706, doi: 10.1175/1520-0493(1982)110<0699:seiteo>2.0.co;2, 1982.

Philander, S. G. H., Yamagata, T. and Pacanowski, R. C.: Unstable Air-Sea Interactions in the Tropics, J. Atmos. Sci., 41(4), 604-613, doi: 10.1175/1520-0469(1984)041<0604:UASIIT>2.0.CO;2, 1984.

Rasmusson, E. M. and Wallace, J. M.: Meteorological aspects of the El Niño/Southern Oscillation, Science, 222(4629), 1195-1202, doi:10.1126/science.222.4629.1195, 1983.

Ropelewski, C. F. and Halpert, M. S.: Global and regional scale precipitation patterns associated with the El Niño/southern Oscillation, Mon. Wea. Rev., 115(8), 1606-1626, doi:10.1175/1520-0493(1987)1152.0.CO;2, 1987.

Rayner, N. A., Parker, D. E., Horton, E. B., Folland, C. K., Alexander, L. V., Rowell, D. P., Kent, E. C. and Kaplan, A.: Global analyses of sea surface temperature, sea ice, and night marine air temperature since the late nineteenth century, J. Geophys. Res., 108(D14), 4407 doi:10.1029/2002JD002670, 2003.

Rao, S. A., Masson, S., Luo, J. J., Behera, S. K. and Yamagata, T.: Termination of indian ocean dipole events in a coupled general circulation model, J. Climate, 20(13), 3018-3035, doi:10.1175/JCLI4164.1, 2007.

Suarez, M. J. and Schopf, P. S.: A delayed action oscillator for ENSO, J. Atmos. Sci., 45(21), 3283-3287, doi: 10.1175/1520-0469(1988)045<3283:adaofe>2.0.co;2, 1988.

Saji, N. H., Coswami, B. N., Vinayachandran, P. N. and Yamagata, T.: A dipole in the tropical Indian Ocean, Nature, 401(6751), 360-363, doi:10.1038/43854, 1999.

Shen, X. S., Kimoto, M., Sumi, A., Numaguti, A. and Matsumoto, Jun.: Simulation of the 1998 East Asian Summer Monsoon by the CCSR/NIES AGCM. J Meteor Soc Japan, 79(3), 741-757, doi:10.2151/jmsj.79.741, 2001.

Saji, N. H. and Yamagata, T.: Possible impacts of Indian Ocean dipole mode events on global climate, Climate Research, 25(2), 151-169, doi: 10.3354/cr025151, 2003.

Taylor, K. E.: Summarizing multiple aspects of model performance in a single diagram, Journal of Geophysical Research: Atmospheres, 106(D7), 7183-7192, doi:10.1029/2000jd900719, 2001.

Ueda, H. and Matsumoto, J.: A possible triggering process of East–West asymmetric anomalies over the Indian Ocean in relation to 1997/98 El Niño, J. Meteor. Soc. Japan, 78(6), 803-818, doi:10.2151/jmsj1965.78.6_803, 2000.

Wyrtki, K.: El Niño-The Dynamic Response of the Equatorial Pacific Ocean to Atmospheric Forcing, J. Phys. Oceanogr., 5(4), 572-584, doi:10.1175/1520-0485(1975)005<0572:entdro>2.0.co;2, 1975.

Webster, P. J. and Yang, S.: Monsoon and ENSO: Selectively interactive systems. Quart. J. Roy. Meteor. Soc., 118(507), 877-926, doi:10.1002/qj.49711850705, 1992.

Webster, P. J., Moore, A. M., Loschnigg, J. P. and Leben R. R.: Coupled ocean-atmosphere dynamics in the Indian Ocean during 1997-98, Nature, 401(6751), 356-360, doi: 10.1038/43848, 1999.

Wang, X. and Wang, C. Z.: Different impacts of various El Niño events on the Indian Ocean Dipole, Climate Dyn., 42(3-4), 991-1005, doi: 10.1175/JCLI-D-12-00638.1, 2014.

Yu, L. S. and Rienecker, M. M.: Mechanisms for the Indian Ocean warming during the 1997-98 El Niño, Geophys. Res. Lett., 26(6), 735-738, doi:10.1029/1999GL900072, 1999.

Yang, H. and Li, C. Y.: Effect of the Tropical Pacific-Indian Ocean Temperature Anomaly Mode on the South Asia High, Chinese Journal of Atmospheric Science (in Chinese), 29(1): 99-110, 2005.

Yang, H., Jia, X. L. and Li, C. Y.: The tropical Pacific-Indian Ocean temperature anomaly mode and its effect, Chin. Sci. Bull., 51(23): 2878-2884, doi:10.1007/s11434-006-2199-5, 2006.

Yang, M., Li, X., Zuo, R., Chen, X. and Wang, L.: Climatology and Interannual Variability of Winter North Pacific Storm Track in CMIP5 Models, Atmosphere, 9(3), 79, doi:10.3390/atmos9030079, 2018.

Zhou, G. Q. and Zeng, Q. C.: Predictions of ENSO with a coupled atmosphere–ocean general circulation model, Adv. Atmos. Sci., 18(4), 587-603, doi:10.1007/s00376-001-0047-8, 2001.

Zheng, F., Zhu, J. and Zhang, R. H.: The impact of altimetry data on ENSO ensemble initializations and predictions, Geophys. Res. Lett., 34(13), doi:10.1029/2007gl030451, 2007.

Zheng, X. T., Xie, S. P., Du, Y., Liu, L., Huang, G. and Liu, Q.: Indian Ocean Dipole Response to Global Warming in the CMIP5 Multimodel Ensemble, J. Climate, 26(16), doi:6067-6080, 10.1175/JCLI-D-12-00638.1, 2013.

Zheng, C. W. and Li, C. Y.: Variation of the wave energy and significant wave height in the China Sea and adjacent waters. Renewable and Sustainable Energy Reviews, 43, 381-387, doi:10.1016/j.rser.2014.11.001, 2015.

Zheng, C. W. and Li, C. Y.: Propagation characteristic and intraseasonal oscillation of the swell energy of the Indian Ocean, Applied Energy, 197, 342-353, doi:10.1016/j.apenergy.2017.04.052, 2017.

613